Arteriosclerosis, Thrombosis, and Vascular Biology

ORIGINAL RESEARCH

Untargeted Lipidomics Reveals a Specific Enrichment in Plasmalogens in Epicardial Adipose Tissue and a Specific Signature in Coronary Artery Disease

Magali Barchuk, Anne Dutour, Patricia Ancel, Ljubica Svilar, Veronica Miksztowicz, Graciela Lopez, Miguel Rubio, Laura Schreier, Juan Patricio Nogueira, René Valero, Sophie Beliard, Jean Charles Martin, Gabriela Berg,* Bénédicte Gaborit*

OBJECTIVE: Epicardial adipose tissue (EAT) is an active endocrine organ that could contribute to the pathophysiology of coronary artery disease (CAD) through the paracrine release of proatherogenic mediators. Numerous works have analyzed the inflammatory signature of EAT, but scarce informations on its lipidome are available. Our objective was first to study the differences between EAT and subcutaneous adipose tissue (SAT) lipidomes and second to identify the specific untargeted lipidomic signatures of EAT and SAT in CAD.

APPROACH AND RESULTS: Subcutaneous and EAT untargeted lipidomic analysis was performed in 25 patients with CAD and 14 patients without CAD and compared with paired plasma lipidomic analysis of isolated VLDL (very low-density lipoprotein) and HDL (high-density lipoprotein). Lipidomics was performed on a C18 column hyphenated to a Q-Exactive plus mass spectrometer, using both positive and negative ionization mode. EAT and SAT had independent lipidomic profile, with 95 lipid species differentially expressed and phosphatidylethanolamine 18:1p/22:6 twenty-fold more expressed in EAT compared with SAT false discovery rate $=3\times10^{-4}$). Patients with CAD exhibited more ceramides (P=0.01), diglycerides (P=0.004; saturated and nonsaturated), monoglycerides (P=0.013) in their EAT than patients without CAD. Conversely, they had lesser unsaturated TG (triglycerides; P=0.02). No difference was observed in the 295 lipid species found in SAT between patients with and without CAD. Fifty-one lipid species were found in common between EAT and plasma lipoproteins. TG 18:0/18:0/18:1 was found positively correlated (r=0.45, P=0.019) in EAT and HDL and in EAT and VLDL (r=0.46, P=0.02).

CONCLUSIONS: CAD is associated with specific lipidomic signature of EAT, unlike SAT. Plasma lipoprotein lipidome only partially reflected EAT lipidome.

Key Words: adipose tissue ■ coronary artery disease ■ lipidomics ■ lipoprotein ■ mass spectrometry

The prevalence of obesity and type 2 diabetes mellitus has considerably increased these recent years. These metabolic diseases are strongly associated with cardiovascular diseases, contributing to global mortality burden.[1] Organ-specific adiposity has renewed growing interest in that it probably contributes to the pathophysiology of cardiometabolic diseases.[2] However, the molecular changes in adipose tissue that promote these disorders are not completely understood and, in particular, the specific role of cardiac adiposity. Epicardial adipose tissue (EAT) is the visceral fat deposit over the heart, located between the myocardium and the visceral pericardium.[3] Over the last years, the perception of this ectopic fat depot has evolved. EAT is more than a simple

Correspondence to: Bénédicte Gaborit, Endocrinology, Metabolic Diseases and Nutrition Department, Pole ENDO, Hôpital Nord, Chemin des Bourrely, 13915 Marseille cedex 20, France. Email benedicte.gaborit@ap-hm.fr

*These authors contributed equally to this article.

The online-only Data Supplement is available with this article at https://www.ahajournals.org/doi/suppl/10.1161/ATVBAHA.120.313955.

For Sources of Funding and Disclosures, see page xxx.

Arterioscler Thromb Vasc Biol is available at www.ahajournals.org/journal/atvb

Nonstandard Abbreviations and Acronyms

CAD	coronary artery disease
Cer	ceramide
DG	diglycerides
EAT	epicardial adipose tissue
HDL	high-density lipoprotein
IL	interleukin
LDL	low-density lipoprotein
MCP-1	monocyte chemotactic protein-1
MS	mass spectrometry
PLS	partial least squares
SAT	subcutaneous adipose tissue
TG	triglycerides
TNF	tumor necrosis factor
TRL	TG-rich lipoproteins remnants
VLDL	very-low-density lipoprotein

Highlights

- Epicardial adipose tissue (EAT) has an independent lipidomic profile compared to subcutaneous adipose tissue.
- We uniquely report a specific enrichment in phosphatidylethanolamine, phosphatidylcholine, short- and medium-chain fatty acids in TG (triglyceride) in the EAT compared to subcutaneous adipose tissue. EAT showed an increase in plasmalogens that could reflect a specific thermogenic activity compared to subcutaneous adipose tissue.
- In coronary artery disease, EAT had a specific lipidomic signature with a significant increase in proinflammatory lipids, such as sphingolipids (ceramides), diglycerides and monoglycerides, and a decrease, in unsaturated TG, in contrast to subcutaneous adipose tissue.
- Plasma lipoprotein (HDL [high-density lipoprotein] and VLDL [very low-density lipoprotien]) lipidome only partially reflected EAT lipidome.

fat storage depot. Indeed, it is now widely recognized to be an extremely active endocrine organ, producing cytokines, adipokines, chemokines that could either be protective or harmful depending on the local microenvironment.[4,5] This richness probably highlights the complex cellularity and cross-talk between EAT and neighboring structures. EAT metabolism is uniquely regulated because of high basal rates of fatty acid uptake, insulin-induced lipogenesis, and high fatty acid breakdown.[6] EAT may act as a local energy store for cardiac muscle and has a protective role against elevated levels of free fatty acid in the coronary circulation.[7] However, amount and type of fatty acids stored could also play a role in the onset and development of atherosclerosis. Interestingly, some gas-liquid chromatography based studies showed an increase in some saturated (C14:0, C16:0, and C18:0) and conjugated linoleic fatty acids and a decrease in unsaturated fatty acids in EAT of patients with type 2 diabetes mellitus.[8,9] Recent studies have shown that the volume of epicardial fat was strongly positively correlated with the presence of coronary artery disease (CAD) and predicted future coronary events at 8 years.[10,11] However, there is scarce information about the lipidome differences between EAT and subcutaneous adipose tissue (SAT) of patients with CAD and the comparison with the lipidome of TRL (TG-rich lipoproteins remnants), and HDL (high-density lipoprotein).

Unlike genes and proteins, metabolites serve as direct signatures of biochemical activity, being, therefore, easier to correlate with the phenotype. In this context, metabolomics and its derivative lipidomics have become powerful approaches opening a window to mechanistically investigate how biochemistry relates to clinical phenotype.[12,13] Targeted and untargeted lipidomics are the 2 main techniques applied for lipid species analyses of various biological samples, including adipose tissue. The targeted approach aims to identify specific groups of lipids selected beforehand while untargeted analysis characterizes overall detectable lipid content. Therefore, the aim of this study was to identify the specific untargeted lipidomic signature of EAT in the context of CAD and to compare it with the plasma lipidomic signature of TRL.

MATERIAL AND METHODS

The data that support the findings of this study are available from the corresponding author upon reasonable request.

Patients

The study included 39 consecutive patients undergoing coronary artery bypass graft (n=25) or valve replacement (n=14) at the Cardiac Surgery Division of Hospital de Clinicas José de San Martín, University of Buenos Aires. All patients gave written informed consent, and the study was approved by the Ethical Review Committee of the Faculty of Pharmacy and Biochemistry, University of Buenos Aires and by the Ethical Review Committee of the Hospital de Clínicas José de San Martín. Paired adipose tissue samples were obtained from thoracic subcutaneous (parasternal region) and EAT (at the origin of the right coronary artery) during elective surgical procedure and before the extracorporeal circulation was started. Samples were washed, fragmented, and immediately flashfrozen in liquid nitrogen before being stored at −80°C. Clinical data were obtained upon admission to the hospital before surgery. Diagnosis of CAD was based on coronarography. Reductions in luminal coronary artery diameters >70% were considered significant. Previous diagnosis of type 2 diabetes mellitus was assessed according to the American Diabetes Association.[14] Patients without CAD were randomly selected among patients who did not undergo coronary artery bypass graft intervention.

These patients had no clinical signs of CAD and showed normal coronary arteries on angiography. The weight and height of each participant were measured, and body mass index and blood pressure were recorded in all cases. The following exclusion criteria were considered for both groups: previous heart surgery, concomitant infective diseases, alcohol intake >20 g/d, recent history of acute illness, end-stage organ failure, and any other condition that may interfere with the results.

VLDL and HDL Isolation

VLDL (density <1.006 g/mL) and HDL (density: 1.063–1.210 g/mL) were isolated by sequential preparative ultracentrifugation in a Beckman XL-90 using a fixed-angle rotor type 90 Ti at 105.000*g*, for 18 hours, at 18°C and 4°C, respectively.[15] Purity of lipoproteins was tested by agarose gel electrophoresis, as previously described.[16]

Determination of Lipidomic Profile

Lipid Extraction

For lipid extraction, methyl-terbutyl ether was used as the extraction solvent, as fully described by Matyash et al.[17] A volume of 200 µL of VLDL fraction, 400 µL of the HDL fraction was extracted. Before extraction, 10 mg of adipose tissue (EAT or SAT) were cut in small pieces.

Briefly, 1.5 mL of methanol and 5 mL of methyl-terbutyl ether were added to each sample and vortexed for 1 hour. Subsequently, 1.25 mL of deionized water was added to each tube and incubated for 10 minutes at room temperature, after homogenization. The tubes were then centrifuged for 10 minutes at 1000 rpm and 10°C, and the upper organic phase was separated in another tube. The lower phase was washed with 2 mL of a methyl-terbutyl ether /methanol/water mixture (20:6:5, v/v/v) and centrifuged as previously described for a second extraction. The upper organic phase was pooled with the first one obtained in previous step. Solvent was evaporated under a stream of nitrogen and dried lipid extract were stored at −80°C until processing. Lipid extracts were then resuspended in 200 µL of a chloroform/methanol/distilled water mixture (40:20:3, v/v/v).

Liquid Chromatography

The UHPLC separation was performed on a DionexUltiMate 3000 device (Thermo Fisher Scientific, Courtaboeuf, France) using the Accucore C18 column (150×2.1 mm, 2.6 µm).

The column temperature was kept at 45°C. Mobile phase A contained 10 mmol/L ammonium formate in 60% acetonitrile and 0.1% formic acid, and mobile phase D contained a 10 mmol/L ammonium formate in acetonitrile:propan-2-ol (1:9, v/v) mixture with 0.1% formic acid. The flow rate was 0.4 mL/min. The elution gradient was: 35% D at the beginning, 35% to 60% D for 4 minutes, 60% to 85% B for 8 minutes, 85% to 100% B for 9 minutes, 100% B for 3 minutes, and 35% B for 4 minutes. The injection volume was 2 µL.

Samples were randomly assigned to the injection table and interspaced (1 of 5) with quality control samples made up of a pool of each sample or solvent for blank. All samples were analyzed in a single series for HDL and VLDL or EAT and SAT.

Mass Spectrometry

Mass spectrometry (MS) spectra of the analyzed samples were acquired using a Q-Exactive Plus (Thermo Fisher) spectrometer with electrospray ionization in positive and negative modes and with a full scan (m/z 250 to 1200) according to the methodology detailed by Breitkopf et al.[18] Briefly, the drying temperature was set to 285°C, the capillary voltage was set to 3000 V. The resolution of the orbitrap mass analyzer was set to of 4 scans/s at 35 000 resolution and injection time of 200 ms.

Full MS spectra were acquired for each sample. Data Dependent Analysis Top 15 MS/MS were used for the acquisition of the MS/MS spectra and performed in one-tenth of the samples. Each sample was acquired in positive and negative ionization modes separately to obtain as much structural information as possible. This method consists in detecting the most abundant ionic species in the primarily acquired full MS spectra. These 15 ionic species are consequently fragmented by higher collision-induced dissociation in the next 15 scans finishing the cycle with the last MSMS. New cycle starts with a new full MS scan and another 15 MS/MS scans for the next 15 ionic species.

Data Treatment

Once the data of the molecular ions corresponding to the metabolites were acquired, the resulting spectra were visually inspected to control the signal intensity. The acquired spectra were divided into 2 groups:

Spectra used for the creation of a data matrix, for use in the XCMS software: the 3-dimensional raw data (m/z, retention time and ion intensity) obtained from the liquid chromatography-MS analysis were deconvolved in a composite matrix of chromatographic peaks aligned in time and a mass-to-charge ratio (m/z) with the intensity of the respective ions. Proteo Wizard MS Convert software was used to convert the original data files (*.raw) into more interchangeable formats and centroid mode (*.mzXML) for both analyzed positive and negative spectra. Data processing were performed using the open-source XCMS software as previously described.[19]

Peak detection was achieved using the centWave method. Maximum and minimum peak width were 2 and 60 seconds, S/N threshold was maintained at 3, where the noise was 12 000 for positive and 6000 for negative ionization mode, difference of m/z at −0.00005, maximal deviation of m/z in 2 consecutive scans 5 ppm. Detection of peak in 4 consecutive scans with minimal intensity 60 000 was considered as a real peak. Peak alignment between samples was achieved using the Obiwarp method and for grouping peaks method density was applied.

Once the matrix of raw data was obtained, several filters were applied to eliminate the analytical background and correct the analytical drift. All signals from electronic noise, as well as null samples, were removed manually. Unstable peaks and redundant information (fragments, adducts, and isotopes) were eliminated by using the coefficients of variation of the peaks applied to the control samples.

Spectra used to create a database using LipidSearch software (v4.0, Thermofischer scientific): an in silico database was built using LipidSearch software, based on the MS/MS spectra recorded in the samples. This software contains the in silico database of different lipid families, based on their specific fragmentation mode and the length of the FA chains. This theoretical fragmentation model corresponds to the MS/MS spectra of the tissue extracts, and the annotations of various fragmented ions were made based on the m/z ratio of the parent ions and the fragments created.

In most of the signals, it was possible to identify the corresponding lipid species. Once the lipids in the LipidSearch matrix were identified, the resulting m/z and retention time pairs were matched to that of obtained with XCMS using the data inhouse tool of the Galaxy Workflow4Metabolomics web application,[20] to identify the lipid species and their intensities in each sample. A final filter was applied to this last database, using parameters such as relative SD, duplicates in both modes, choice of the most stable, and most intense peak for each lipid among others. This curated and annotated matrix containing semi-quantitative value for each lipid per sample was used for statistical analyses.

Statistical Analysis

Anthropometric and biochemical parameters were expressed as mean ± SD or median and 25th to 75th percentile. Lipid species relative quantification was expressed in percentages ± SEM. Principal component analyses, partial least squares (PLSs), and orthogonal PLSs regression analyses of autoscaled values were performed with Simca P12 software (Sartorius Stedim Biotech, Göttingen, Germany) or MetaboAnalyst (http://www.metaboanalyst.ca/)[21] and GraphPad Prism 6.0. Pathways enrichment was performed with MetaboAnalyst using small molecule pathway database. Cooman plot analysis was performed to determine the effect of gender on the EAT lipidome. Class membership was tested against the 2 principal component analyses models in a SIMCA procedure. The distance from each model is computed (DmodX1 and DmodX2, respectively) and plotted. The Dcrit value for each model defines the class. Thus, there were 4 possible outcomes: an individual could be predicted to be males, females only, neither or both (eg, undefined). The gaussian distribution of the data sets was assessed by Shapiro-Wilk normality test. The significant differences between groups were detected by Student 2-sample *t* test or Wilcoxon rank-sum test when appropriate. The Benjamini Yekutieli procedure for controlling the false discovery rate was applied. $P<0.05$ was considered statistically significant.

Table 1. Characteristics of the Studied Population

Parameters	NCAD (n=14)	CAD (n=25)	*P* Value
Age, y	64.1±14.4	63.8±11.3	NS
Sex, n (% men)	7 (50)	23 (92)	0.005
Body mass index, kg/m²	29.9±6.6	28.6±4.6	NS
Hypertension, n (%)	9 (64)	17 (68)	NS
Ex-smokers, n (%)	2 (14)	12 (48)	0.044
Systolic blood pressure, mm Hg	120±19	132±18	NS
Diastolic blood pressure, mm Hg	60 (60–72)	71 (60–80)	NS
Atrial fibrillation, n (%)	0 (0)	1 (4)	NS
Valvular disease, n (%)	14 (100)	0 (0)	<0.001
Aortic/mitral	12 (85)/2 (15)		
Stenosis/insufficiency	8 (57)/6 (43)		
Biological parameters			
Glycemia, g/L	0.90 (0.85–0.94)	1.07 (0.94–1.37)	<0.001
hsCRP, mg/L	0.61±0.21	2.96±1.41	<0.001
Uric acid, µmol/L	293.7±53.1	289.4±83.9	NS
GFR (CKD-EPI), mL/min	80.1±13.4	89.3±13.6	NS
Lipid profile, g/L			
Total cholesterol	1.35 (1.04–1.73)	1.21 (1.01–1.37)	NS
Triglycerides	0.93 (0.64–1.39)	1.37 (0.95–1.73)	0.040
LDL-cholesterol	1.00 (0.67–1.30)	0.72 (0.53–0.86)	NS
HDL-cholesterol	0.38 (0.30–0.44)	0.30 (0.25–0.39)	NS
Non–HDL-cholesterol	0.96 (0.71–1.37)	0.85 (0.65–0.98)	NS
TG-rich lipoproteins	0.08 (0.04–0.11)	0.17 (0.08–0.21)	0.001
Lipid ratio (total Chol/HDL Chol)	3.43 (2.99–4.92)	4.03 (3.10–4.68)	NS

CAD indicates coronary artery disease; HDL, high-density lipoprotein; LDL, low-density lipoprotein; NCAD, non-coronary artery disease; NS, not significant; and TG, triglyceride.

RESULTS

Thirty-nine patients were included (25 CAD and 14 non-CAD) patients with a mean age of 63.8±11.3 years (CAD group) versus 64.1±14.4 years (non-CAD group, *P*=NS) and a mean body mass index of 28.6±4.6 (CAD) versus 29.9±6.6 kg/m² (non-CAD), respectively (*P*=NS). As expected, patients with CAD had more cardiovascular risk factors than patients without CAD (Table 1).

Representative MS/MS spectra for one CAD and one non-CAD subject in EAT, SAT and associated extracted chromatograms of 4 representative lipids are shown in Figure I in the Data Supplement. Two-hundred and ninety-five lipid species were identified in the adipose tissues, with as expected TGs (triglycerides) as the major component (96.8% of lipid species for EAT and SAT).

Differences Between Epicardial and SAT Lipidomes

A PLS regression calculated between paired EAT and SAT total lipidomic profiles (n=39 whole group) showed no significant overarching relationships between the 2 adipose tissues. In addition, orthogonal PLS paired statistics showed that EAT and SAT had a totally different lipidomic profile (Figure 1), with 95 lipid species differentially expressed between the 2 adipose tissues (false discovery rate <0.05; Table 2). The samples were well separated with respect to adipose tissue location, the latter explaining 62% of lipid species variance (Figure 1). In particular, phosphatidylethanolamine 18:1p/22:6 was >20-fold expressed in EAT compared with SAT, false discovery rate 3×10^{-4} (Table 2). EAT had also the highest content in C20/C22 polyunsaturated fatty acids lipid species, including C22:6n-3 containing lipids. It was also wealthier in unusual adipose short (C4/C6) to medium (C10/C12) chain saturated fatty acids TG species than SAT. Conversely, EAT had the lowest content in C18:1 and C18:2 fatty acids TGs, as well as in less usual adipose very long-chain (>C20–C28) saturated fatty acids (Table 2).

An increase in sphingolipids (ceramides [Cer d18:2/18:0, Cer d18:1/18:0, and Cer d18:1/24:1] and sphingomyelin [sphingomyelin d41:1]) was observed in

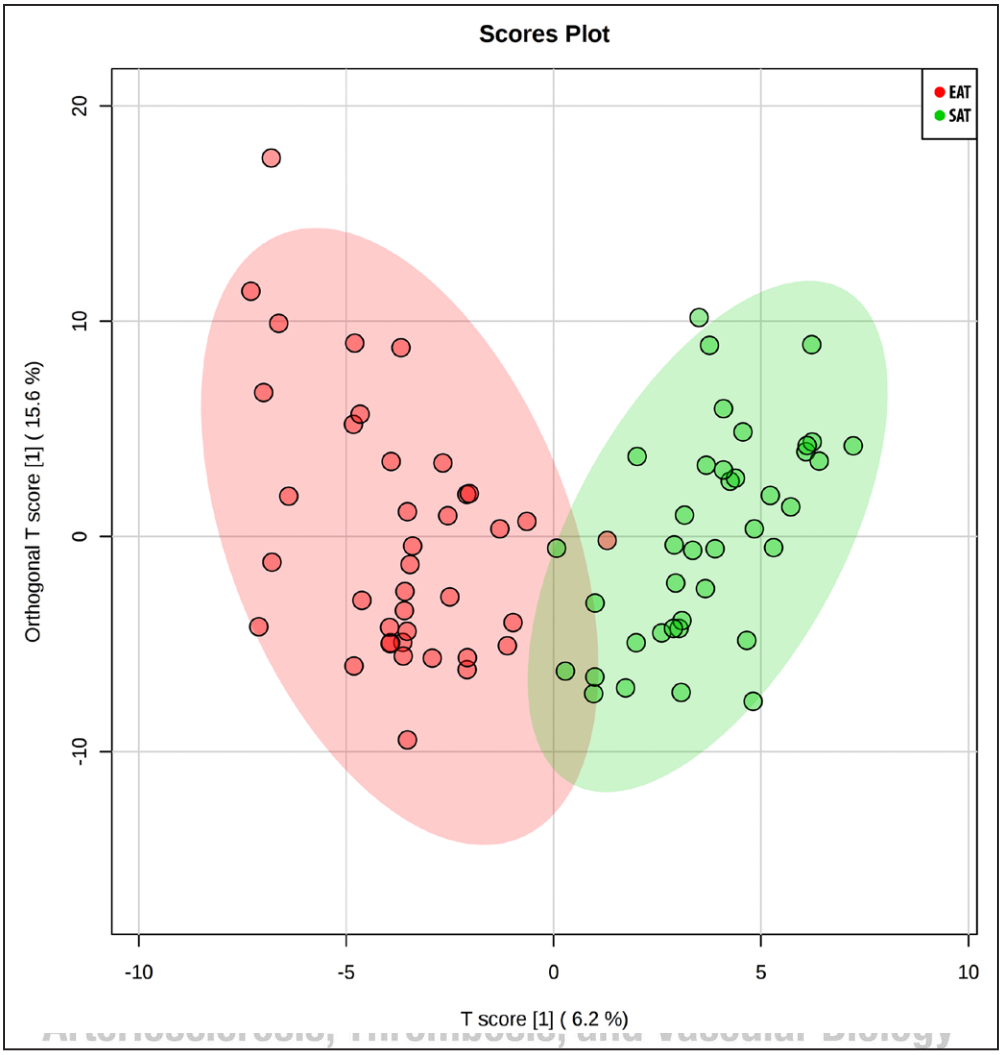

Figure 1. Orthogonal partial least squares (O-PLS) graph demonstrating a differential effect of adipose tissue location (epicardial adipose tissue [EAT] versus subcutaneous adipose tissue [SAT]) on lipidomic profiles.
Red spots represent samples from epicardial adipose tissue EAT and green spots represent samples from subcutaneous adipose tissue. Model cross-validation results: R2=0.62. Q2=0.483. Permutation test validation (2000 repetitions) $P<5\times10^{-4}$.

EAT compared with SAT (P=0.02 and P=0.005). EAT was 3-fold richer in glycerophosphatidylcholines (P<0.001) and 2-fold richer in glycerophosphatidylethanolamines (P<0.001) compared with SAT. By contrast, a significant decrease in monoglycerides and Coenzyme-Q6 was observed in EAT versus SAT (Figure 2). No difference was observed for other glycerolipids and for the saturated of fatty acids. No correlation was found between lipid species of EAT and SAT.

Likewise, pathway analysis showed a significant enrichment in sphingolipid metabolism in EAT versus SAT (P<0.001, Figure II in the Data Supplement).

Differences Between SAT Lipidome of CAD and Non-CAD Patients

Using the same methodology, no difference was observed in the 295 annotated lipid species found in the SAT between patients with and without CAD (Figure 3).

Differences Between EAT Lipidome of CAD and Non-CAD Patients

Using PLS approach and variable importance in the projection value, we identified 97 lipid species that discriminated patients with and without CAD (cutoff variable importance in the projection 0.88; Figure 4A and 4B, Table I in the Data Supplement). Among these phosphatidylethanolamine 18:0p/20:4 was the most important. Dendrogram analysis confirmed that patients with and without CAD clustered differently (Figure 4C). Patients with CAD exhibited more ceramides (P=0.01), diglycerides (P=0.004; saturated and nonsaturated), monoglycerides (P=0.013) in their EAT than patients without CAD. Conversely, they had lesser total TGs, mainly unsaturated (P=0.02). Long-chain fatty acids were increased in unsaturated monoglycerides and medium and long-chain fatty acids were found significantly increased in diglycerides in CAD versus non-CAD (all P<0.05).

Table 2. Statistical Paired Analysis Reveals 95 Lipid Species Differentially Expressed Between EAT and SAT in the Whole Group (n=39)

Lipid Species	m/z Ratio	*P* Value	FDR	Fold Change	EAT vs SAT
PE 18:1p/22:6	752.56	1.19×10^{-5}	3.06×10^{-4}	23.72	Up
PE 18:0p/20:4	774.54	3.25×10^{-5}	4.56×10^{-4}	5.44	Up
PE 18:0/20:3	768.55	1.15×10^{-5}	3.06×10^{-4}	4.86	Up
PC 16:0/20:4	782.57	2.03×10^{-5}	3.74×10^{-4}	3.35	Up
DG 37:6	649.48	1.59×10^{-5}	3.14×10^{-4}	3.31	Up
PE 16:0p/20:4	724.53	6.29×10^{-4}	3.87×10^{-3}	3.04	Up
TG 18:1/22:4/22:6	998.82	7.89×10^{-8}	1.16×10^{-5}	2.80	Up
TG 4:0/16:0/22:6	728.58	8.56×10^{-3}	2.94×10^{-2}	2.77	Up
PE 18:0p/18:2	728.56	1.06×10^{-3}	5.28×10^{-3}	2.75	Up
TG 4:0/16:0/18:1	687.55	1.35×10^{-5}	3.07×10^{-4}	2.70	Up
TG 45:4	774.66	2.02×10^{-3}	8.90×10^{-3}	2.63	Up
Cer d18:2/18:0	564.54	6.15×10^{-10}	1.81×10^{-7}	2.61	Up
TG 16:0/8:0/22:6	784.65	3.88×10^{-4}	2.54×10^{-3}	2.54	Up
TG 6:0/16:0/22:6	756.61	1.16×10^{-2}	3.72×10^{-2}	2.53	Up
TG 16:0/22:6/22:6	968.77	7.07×10^{-4}	4.09×10^{-3}	2.49	Up
Cer d18:1/18:0	566.55	1.29×10^{-7}	1.27×10^{-5}	2.40	Up
TG 43:4	746.63	3.20×10^{-3}	1.31×10^{-2}	2.38	Up
TG 11:0/18:2/18:3	800.68	9.97×10^{-4}	5.16×10^{-3}	2.33	Up
TG 17:4/16:1/16:1	826.69	6.25×10^{-3}	2.41×10^{-2}	2.29	Up
TG 47:6	798.66	3.65×10^{-4}	2.50×10^{-3}	2.29	Up
TG 4:0/16:0/17:1	668.58	8.56×10^{-3}	2.94×10^{-2}	2.16	Up
PE 18:0p/18:1	730.57	1.32×10^{-3}	6.47×10^{-3}	2.16	Up
TG 16:0/10:0/22:6	812.68	7.07×10^{-4}	4.09×10^{-3}	2.12	Up
TG 16:0/8:0/20:4	760.65	4.13×10^{-4}	2.65×10^{-3}	2.12	Up
TG 8:0/18:1/20:4	786.66	6.54×10^{-3}	2.41×10^{-2}	2.10	Up
PE 36:1	746.57	1.29×10^{-4}	1.08×10^{-3}	2.06	Up
TG 18:1/22:6/22:6	994.79	5.91×10^{-5}	6.46×10^{-4}	2.06	Up
PE 18:1/18:1	744.55	6.25×10^{-3}	2.41×10^{-2}	2.05	Up
Cer d18:1/24:1	648.63	1.47×10^{-4}	1.21×10^{-3}	2.01	Up
TG 18:0/18:1/22:6	950.82	1.47×10^{-5}	3.10×10^{-4}	1.99	Up
PC 32:2	730.54	7.49×10^{-4}	4.25×10^{-3}	1.99	Up
TG 45:5	772.64	5.19×10^{-3}	2.10×10^{-2}	1.99	Up
TG 16:0/16:0/22:6	896.77	3.78×10^{-5}	4.85×10^{-4}	1.94	Up
Cer d18:0/16:0	540.54	2.50×10^{-4}	1.84×10^{-3}	1.94	Up
TG 22:4/18:2/22:6	996.80	3.51×10^{-5}	4.70×10^{-4}	1.92	Up
Cer d18:2/20:0	592.57	8.91×10^{-4}	4.69×10^{-3}	1.91	Up
TG 16:0/14:0/22:6	868.74	6.84×10^{-5}	6.96×10^{-4}	1.90	Up
TG 14:0/18:2/22:6	892.73	6.54×10^{-3}	2.41×10^{-2}	1.88	Up
SM d41:1	801.68	2.84×10^{-4}	2.04×10^{-3}	1.85	Up
TG 18:0/16:0/22:6	924.80	2.05×10^{-4}	1.64×10^{-3}	1.80	Up
PE 18:0p/22:6	776.56	6.36×10^{-5}	6.70×10^{-4}	1.78	Up
TG 16:0/12:0/22:6	840.71	4.39×10^{-4}	2.75×10^{-3}	1.73	Up
DG 18:0/22:4	690.60	7.94×10^{-4}	4.26×10^{-3}	1.72	Up
TG 18:1/20:3/22:6	972.80	2.09×10^{-6}	1.23×10^{-4}	1.71	Up
PEt 15:0/18:1	689.51	1.47×10^{-3}	6.99×10^{-3}	1.71	Up
TG 16:0/18:1/22:6	922.79	1.25×10^{-5}	3.06×10^{-4}	1.71	Up
TG 6:0/17:1/18:2	720.61	2.34×10^{-4}	1.77×10^{-3}	1.71	Up
TG 9:0/18:2/18:2	774.66	6.54×10^{-3}	2.41×10^{-2}	1.65	Up

(*Continued*)

Table 2. Continued

Lipid Species	m/z Ratio	*P* Value	FDR	Fold Change	EAT vs SAT
TG 15:0/18:1/22:6	908.77	5.91×10^{-5}	6.46×10^{-4}	1.65	Up
TG 16:0/18:2/22:6	920.77	7.49×10^{-6}	2.45×10^{-4}	1.64	Up
TG 18:1/18:1/22:5	950.82	1.06×10^{-2}	3.49×10^{-2}	1.56	Up
TG 18:1/18:2/20:2	926.82	1.20×10^{-4}	1.04×10^{-3}	1.53	Up
TG 52:4e	858.79	5.70×10^{-3}	2.27×10^{-2}	1.52	Up
TG 18:1/18:1/22:3	954.84	3.43×10^{-4}	2.41×10^{-3}	1.51	Up
PE 34:1	718.54	3.20×10^{-3}	1.31×10^{-2}	1.51	Up
TG 16:0e/16:1/18:2	832.78	1.37×10^{-2}	4.30×10^{-2}	1.49	Up
TG 18:0/18:1/22:4	954.85	2.02×10^{-3}	8.90×10^{-3}	1.47	Up
TG 16:0/22:5/22:6	970.79	3.05×10^{-6}	1.50×10^{-4}	1.46	Up
TG 18:2/22:6/22:6	992.77	1.47×10^{-3}	6.99×10^{-3}	1.43	Up
TG 17:0/18:2/22:6	934.78	8.95×10^{-3}	3.03×10^{-2}	1.34	Up
TG 16:0e/18:1/22:5	910.82	6.84×10^{-3}	2.49×10^{-2}	1.33	Up
TG 17:4/12:0/12:0	718.60	1.06×10^{-2}	3.49×10^{-2}	1.31	Up
TG 20:1/18:1/20:2	956.85	9.75×10^{-5}	9.59×10^{-4}	1.12	Up
DG 16:0/20:4	634.54	9.76×10^{-3}	3.27×10^{-2}	1.01	Up
TG 18:2/17:1/18:2	884.77	1.06×10^{-3}	5.28×10^{-3}	0.77	Down
PE 16:0e	454.29	1.64×10^{-3}	7.54×10^{-3}	0.74	Down
DG 14:0/14:0	530.48	2.89×10^{-3}	1.24×10^{-2}	0.70	Down
TG 19:0/18:1/20:1	946.87	1.31×10^{-2}	4.17×10^{-2}	0.68	Down
DG 15:0/18:2	596.53	7.94×10^{-4}	4.26×10^{-3}	0.64	Down
TG 18:3/18:2/18:2	894.75	1.43×10^{-2}	4.44×10^{-2}	0.63	Down
TG 15:0/18:2/18:3	856.74	6.54×10^{-3}	2.41×10^{-2}	0.61	Down
TG 6:0/12:0/18:1	654.57	8.56×10^{-3}	2.94×10^{-2}	0.59	Down
TG 16:0/18:1/23:1	946.88	2.78×10^{-5}	4.11×10^{-4}	0.58	Down
TG 18:1/18:2/22:0	958.88	7.83×10^{-3}	2.78×10^{-2}	0.58	Down
MG 26:4	463.38	7.49×10^{-3}	2.70×10^{-2}	0.57	Down
TG 18:0/18:1/19:0	920.86	4.40×10^{-5}	5.41×10^{-4}	0.54	Down
TG 18:0/16:0/24:0	964.93	1.16×10^{-2}	3.72×10^{-2}	0.45	Down
TG 16:0/18:1/23:0	948.90	2.38×10^{-5}	3.90×10^{-4}	0.44	Down
TG 18:0/16:0/24:1	962.91	2.62×10^{-3}	1.13×10^{-2}	0.42	Down
TG 18:0/18:1/23:0	976.92	1.12×10^{-4}	1.00×10^{-3}	0.40	Down
TG 18:1/18:2/23:0	972.90	9.47×10^{-7}	6.98×10^{-5}	0.40	Down
TG 18:1/18:1/24:0	988.93	7.07×10^{-4}	4.09×10^{-3}	0.39	Down
TG 20:1/18:1/18:1	935.80	1.82×10^{-3}	8.25×10^{-3}	0.38	Down
TG 18:1/18:1/23:0	974.91	6.29×10^{-6}	2.32×10^{-4}	0.37	Down
TG 27:0/18:1/18:1	1030.97	1.05×10^{-4}	9.64×10^{-4}	0.36	Down
TG 26:0/18:1/18:2	1014.94	6.29×10^{-6}	2.32×10^{-4}	0.36	Down
TG 26:1/16:0/18:0	990.94	3.04×10^{-3}	1.28×10^{-2}	0.35	Down
Co Q6	591.44	1.55×10^{-3}	7.26×10^{-3}	0.34	Down
TG 26:1/18:0/18:1	1016.96	7.94×10^{-4}	4.26×10^{-3}	0.34	Down
TG 28:0/18:1/18:1	1044.99	5.11×10^{-5}	6.02×10^{-4}	0.32	Down
TG 25:0/16:0/18:1	976.93	1.05×10^{-4}	9.64×10^{-4}	0.30	Down
TG 25:0/18:0/18:1	1004.96	2.20×10^{-5}	3.82×10^{-4}	0.28	Down
TG 27:0/18:1/18:2	1028.96	3.88×10^{-4}	2.54×10^{-3}	0.25	Down
TG 25:0/16:0/18:0	978.94	2.19×10^{-4}	1.70×10^{-3}	0.24	Down
DG 26:3	496.40	2.57×10^{-5}	4.00×10^{-4}	0.24	Down

Cer indicates ceramide; Chol, cholesterol; Co, co-enzyme; DG, diglycerides; e, ether; EAT, epicardial adipose tissue; MG, monoglycerides; p, plasmalogen; PC, phosphatidylcholine; PE, phosphatidylethanolamine; PG, phosphatidylglycerol; SAT, subcutaneous adipose tissue; SM, sphingomyelin; and TG, triglycerides.

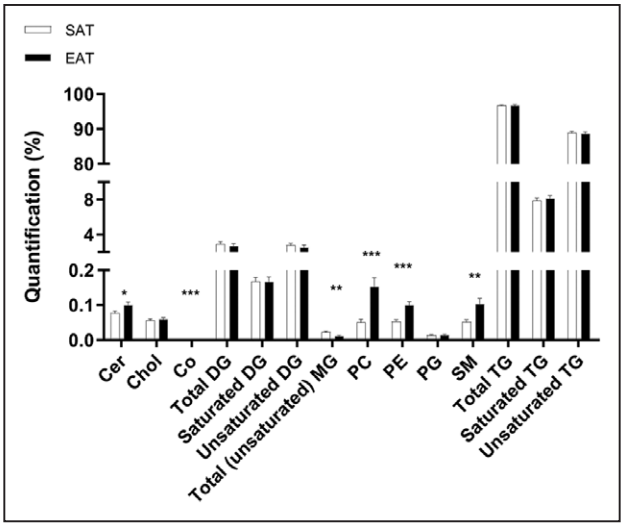

Figure 2. Paired comparison of the lipidomic profile (lipid species) of epicardial versus subcutaneous adipose tissue (n=39).

Cer indicates ceramide; Chol, cholesterol; Co, coenzyme; DG, diglycerides; EAT, epicardial adipose tissue; MG, monoglycerides; PC, phosphatidylcholine; PE, phosphatidylethanolamine; PG, phosphatidylglycerol; SAT, subcutaneous adipose tissue; SM, sphingomyelin; and TG, triglycerides. *P<0.05, **P<0.01, and ***P<0.001.

Remarkably, short-chain fatty acids were observed in TG, mainly represented by caproic acid (TG 6:0/12:0/18:1 and TG 6:0/16:0/17:0). Palmitic acid (16:0) was the fatty acid most represented in TG (Table I in the Data Supplement, Figure 4B and 4D). To further evaluate the effect of gender on EAT lipidome, we performed a Cooman plot analysis. There was no obvious generalization of gender membership (Figure III in the Data Supplement), suggesting that gender effect was not a confounding factor in discriminating EAT lipidome in patients with and without CAD.

Pathway analysis further showed a specific enrichment in phospholipid biosynthesis and glycerolipid metabolism in EAT CAD versus non-CAD patients (both, P=0.006; Figure II in the Data Supplement).

Subgroup Analysis: Comparison of EAT Lipidome to Isolated Lipoproteins (HDL and VLDL) Plasma Lipidome

We further performed a subgroup analysis in 17 patients with CAD and 10 patients without CAD gathering isolated TRL and HDL lipidomics. In patients with CAD, higher content of total lysophosphopholipids lysophosphatidylcholine (P=0.002) and lysophosphatidylethanolamine (P=0.02) in TRL were found. In this lipoprotein, lower content of lysophosphatidylcholine (18:2p; P=0.04) and higher levels of lysophosphatidylcholine (20:4), lysophosphatidylcholine (38:5), and lysophosphatidylcholine (16:0), as well as lysophosphatidylethanolamine (18:1) and lysophosphatidylethanolamine (16:0), were observed in patients with CAD. No differences in the content of lipids in HDL were observed between groups, although patients with CAD presented higher levels of DG (18:1/20:4) and sphingomyelin (22:0/20:2; P=0.04; Figure IV in the Data Supplement).

Only 51 lipid species were found in common between EAT and plasma lipoproteins. Among these species, only 5 lipids were positively correlated between EAT and lipoproteins and were found in the top list of the variable importance in the projection. The most important was TG 18:0/18:0/18:1 (variable importance in the projection 1.58), which was found positively correlated (r=0.45, P=0.019) in EAT and HDL and in EAT and VLDL (r=0.46, P=0.02). TG 16:1/18:1/18:2 was positively correlated in EAT and HDL (r=0.39, P=0.04). TG 16:0/18:1/18:2 was positively correlated in EAT and VLDL (r=0.42, P=0.04).

Plasmalogen Species Analysis

Plasmalogens are a class of membrane glycerophospholipids containing a vinyl-ether linked alkyl chain at the sn-1 position of the glycerol backbone and, typically, a polyunsaturated fatty acyl chain at the sn-2 position. We found 6 plasmalogen species (all phosphatidylethanolamine) in the adipose tissues: phosphatidylethanolamine (16:0p/20:4), phosphatidylethanolamine (18:0p/18:1), phosphatidylethanolamine (18:0p/18:2), phosphatidylethanolamine (18:0p/22:6), phosphatidylethanolamine(18:1p/22:6), and phosphatidylethanolamine (18:0p/20:4) and 17 in the isolated lipoproteins (6 phosphatidylcholine and 11 phosphatidylethanolamine; Figure 5).

Remarkably, we found that plasmalogen species were significantly enriched in EAT compared with SAT in paired analysis. No difference was observed in CAD versus non-CAD patients for EAT, SAT, or plasma isolated lipoproteins (Figure 5).

DISCUSSION

The present study sheds new light on the lipidomic signature of EAT in the context of CAD. We observed a marked difference in the lipidome of adipose tissues depending on their epicardial or subcutaneous origin. EAT and SAT had a totally different lipidomic profile, with 95 lipid species differentially accumulated between the 2 tissues. A specific enrichment in sphingolipids (ceramides with 18 carbons, sphingomyelin), phosphatidylcholine, phosphatidylethanolamine, and phosphatidylethanolamine plasmalogens was observed in EAT compared with SAT. Furthermore, we observed a specific lipidomic signature of EAT in CAD compared to non-CAD patients, in contrast to SAT. We uniquely identified 97 lipid species that discriminated patients with and without CAD. Patients with CAD exhibited more ceramides, diglycerides, monoglycerides, and less unsaturated TGs in their EAT than patients without CAD. Finally, we observed that the EAT

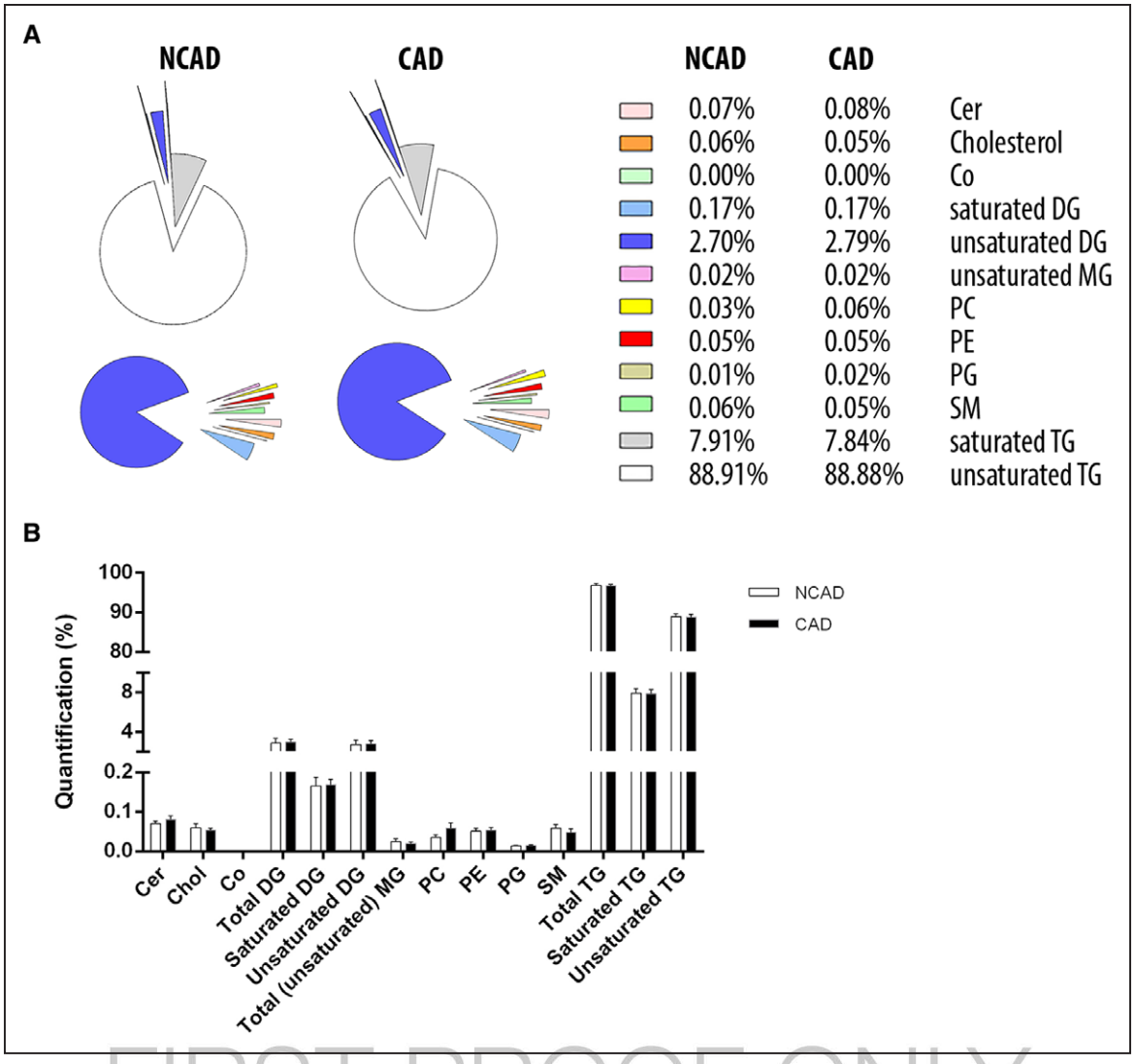

Figure 3. Unpaired comparison of the lipidomic signature of subcutaneous adipose tissue in coronary artery disease (CAD) and non-CAD patients.

Cer indicates ceramide; Chol, cholesterol; Co, co-enzyme; DG, diglycerides; MG, monoglycerides; PC, phosphatidylcholine; PE, phosphatidylethanolamine; PG, phosphatidylglycerol; SM, sphingomyelin; and TG, triglycerides. **P*<0.05, ***P*<0.01, and ****P*<0.001.

lipidome was only partially reflected by the plasma lipoproteins (HDL and VLDL) lipidome. Only 51 lipid species were found in common between EAT and plasma lipoproteins, and only 5 lipid species were correlated between EAT and isolated plasma VLDL or HDL.

Importantly, we found that the EAT lipidome was independent to that of SAT, that could indicate a specific high metabolic activity, or a beige associated phenotype. This is also illustrated by differences in the content of specific lipid species. It concentrated more C20 polyunsaturated lipid species, less C18 unsaturated ones, and less very long-chain saturated fatty acids. This underlined a different metabolic activity, such as desaturation and elongation, or esterification. The presence of higher content in short- to medium-chain saturated fatty acids is also noteworthy. These fatty acids are excellent substrate for mitochondrial β-oxidation since they bypassed the carnitine transport step into the mitochondria.[22] Their higher content in EAT could be thus helpful to deliver a rapid and efficient source of energy to the myocardium. Furthermore, the significant increase of phosphatidylethanolamine plasmalogen species in EAT is remarkable in that recent work from Park et al,[23,24] nicely demonstrated that peroxisome-derived lipids, such as plasmalogens, are able to regulate adipose thermogenesis by mediating cold-induced mitochondrial fission. In this work, inhibition of peroxisomal biogenesis through adipose-specific knockout of the peroxisomal biogenesis factor Pex16 impaired cold-induced mitochondrial fission and resulted in severe cold intolerance and increased diet-induced obesity. Mechanistically, these effects were caused by impaired peroxisomal synthesis of ethanolamine plasmalogens. Since EAT has been shown to exhibit a beige signature,[25,26] with a

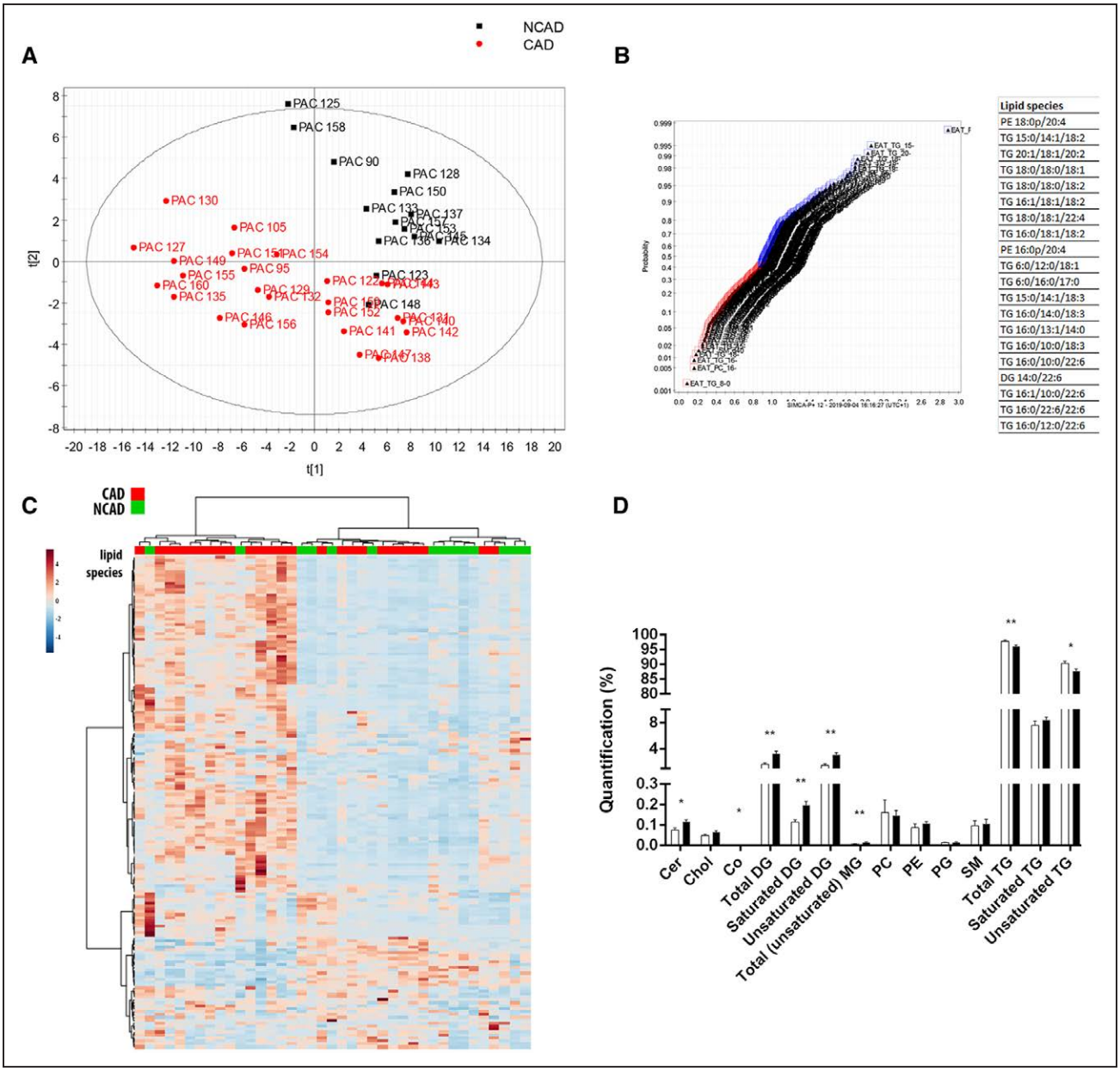

Figure 4. Unpaired comparison of the lipidomic signature of epicardial adipose in coronary artery disease (CAD; n=25) and non-CAD patients (n=14).

A, Partial least squares (PLS)-DA obtained from selected lipid species with variable importance in the projection (VIP) value greater than 0.88, PLS-DA validation with permutation test $P<0.001$. **B**, Selection of lipid species from the VIP values at the inflection point of the curve, VIP value cutoff=0.88–Top 20 VIP lipid species in patients with CAD. **C**, Heatmap representation of hierarchical clustering of molecular features found in each sample of epicardial adipose tissue (EAT) of patients with and without CAD. Red, patients with CAD; green, patients without CAD. Coloration by lipid species abundance intensity in arbitrary units. **D**, Relative quantification of lipid families in EAT of patients with and without CAD.

2-fold increase in PRDM-16 and PGC-1α, one could hypothesize that phosphatidylethanolamine plasmalogens may be implicated in brown activation of EAT through the regulation of mitochondrial dynamics, but this deserves further investigation.

With respect to lipid quantification, adipose tissues are particularly challenging because of their high content of neutral lipids (>99% of triacylglycerols and cholesterol esters) that causes high ion suppression of less abundant membrane lipids.[27] TGs are located in adipocyte lipid droplets, which are dynamic organelles related to vesicle trafficking, cell signaling, and crucial for lipid homeostasis.[28] Up to date, wide-scale lipid profiling has been difficult to assess because the diversified physical properties of lipid metabolites require a variety of purification systems. The evolution of lipidomics has driven the development of new analytic platforms, specifically in the area of MS, that have allowed many more lipid

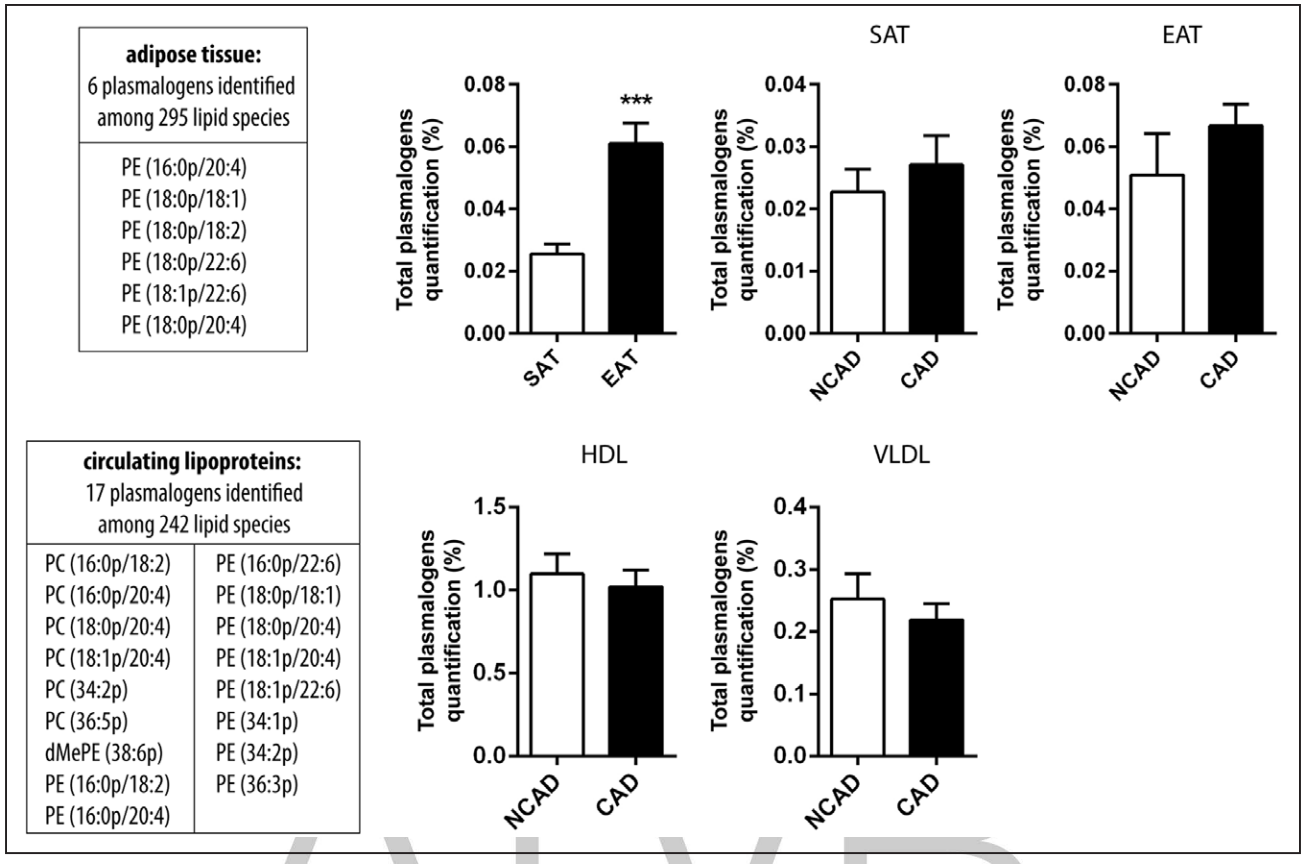

Figure 5. Comparison of the plasmalogen lipidomic profile in adipose tissue (n=39) and isolated lipoproteins (HDL [high-density lipoprotein] and VLDL [very low-density lipoprotein], n=27).
Paired comparison between subcutaneous vs epicardial adipose tissue (SAT vs EAT); unpaired comparison between SAT and EAT in coronary artery disease (CAD) and non-CAD patients; unpaired comparison between plasma isolated HDL or VLDL in CAD and non-CAD patients. dMePE indicates phosphatidyl(dimethyl-ethanolamine); PC, phosphatidylcholine; and PE, phosphatidylethanolamine, ***P<0.001.

species to be analyzed in detail.[13] Recently, Tomášová et al,[29] performed minor lipids profiling in subcutaneous and epicardial fat of 10 patients with CAD tissue using liquid chromatography-MS with detachment of TG by thin-layer chromatography. With this novel preanalytical step, they detected only 37 lipids. Besides, a higher content of phosphatidylcholine and a decreased level of phosphatidylethanolamine (18:0/20:4) was found in EAT compared with SAT; the authors interpret this result as a smaller lipid droplet formation in EAT, as phosphatidylcholine/phosphatidylethanolamine ratio is essential for the size of the monolayer of phospholipids that covers the lipid droplet.[29] Conversely, we observed an increased content in phosphatidylcholine and phosphatidylethanolamine in EAT versus SAT, which may reflect a high proportion of cells membranes in EAT.[30] Our observation is in agreement with histological studies showing that epicardial adipocytes were significantly smaller than those in subcutaneous and peritoneal fat.[31]

Lipidomics of adipose tissues is receiving increasing attention, and previous studies have provided convincing evidence of the dynamic nature of these tissues, deciphering the complex interplay between intratissue bioactive lipids composition such as DG and ceramides and insulin resistance or type 2 diabetes mellitus.[32,33] However, EAT often seen as a visceral proxy, is also a unique pericoronary fat depot with a high lipogenic and lipolytic activity that could play a pivotal role in atherogenesis.[34] In a recent meta-analysis including >40 000 low-to-intermediate cardiovascular risk subjects, EAT volume was independently associated with coronary artery stenosis, myocardial ischemia, and major adverse cardiovascular events.[35] EAT in CAD displays a proinflammatory phenotype, with high levels of reactive oxygen species and a specific pattern of microRNA.[3] Epicardial adipocytes have intrinsic atherogenic and proinflammatory secretion profiles.[36,37] Evaluating the content of bioactive lipids within EAT in the context of CAD was, therefore, crucial. In 2003, Mazurek et al[4] showed that EAT exhibited significantly higher levels of chemokines (ie, MCP [monocyte chemotactic protein]-1) and several inflammatory cytokines IL (interleukin)-6, TNF (tumor necrosis factor)-α, and IL-1β than SAT in patients with CAD.[4] The presence of these inflammatory mediators was hypothesized to accentuate plaque instability via apoptosis (TNF-α), vascular inflammation, and neovascularization (MCP-1). Periadventitial application of endotoxin, MCP-1, IL-1β, or oxidized LDL (low-density lipoprotein) induces inflammatory cell influx into the arterial wall,

Table 3. Pearson or Spearman Correlation Between Common Lipids Found in Isolated Plasma HDL/VLDL Versus EAT (n=27 Patients, 17 CAD and 10 NCAD Patients)

	EAT vs HDL		EAT vs VLDL		EAT CAD vs NCAD	EAT CAD vs NCAD
Lipid Species	r	*P* Value	r	*P* Value	Regulation	Significative VIP
PE 18:0p/20:4	0.19	0.332	0.27	0.201	Up	2.29
TG 18:0/18:0/18:1	0.45	0.019	0.46	0.024	Up	1.58
TG 16:1/18:1/18:2	0.39	0.043	0.19	0.366	Up	1.52
TG 16:0/18:1/18:2	0.04	0.849	0.42	0.041	Down	1.47
PE 16:0p/20:4	0.01	0.974	0.10	0.642	Up	1.45
TG 16:0/17:0/18:1	−0.21	0.296	−0.22	0.302	Up	1.21
TG 18:0/17:0/18:1	0.36	0.065	0.37	0.076	Up	1.10
TG 18:0/16:0/18:1	−0.18	0.370	−0.11	0.599	Down	1.08
PE 18:0/20:3	0.10	0.615	0.12	0.578	Up	1.08
TG 15:0/18:2/18:3	0.39	0.047	−0.02	0.929	Up	1.03
TG 18:0/16:0/16:0	−0.27	0.182	−0.28	0.192	Down	0.97
TG 18:1/18:1/18:2	0.04	0.835	0.27	0.209	Down	0.97
DG 16:0/18:1	−0.06	0.753	−0.20	0.351	Up	0.96
TG 18:2/18:2/22:6	0.35	0.072	0.24	0.260	Up	0.93
DG 16:0/16:0	−0.04	0.842	−0.06	0.768	Up	0.93
DG 18:0/16:0	0.27	0.180	0.23	0.284	Up	0.92
DG 18:1/18:2	−0.23	0.239	−0.21	0.330	Up	0.92
DG 18:1/20:4	0.14	0.475	0.20	0.360	Up	0.92
TG 16:0/18:1/22:6	0.60	0.001	0.65	0.001	Up	0.91
DG 18:0/18:1	−0.17	0.399	−0.17	0.419	Up	0.90
Cer d18:1/24:1	0.13	0.522	−0.07	0.759	Up	0.90
TG 15:0/18:1/22:6	0.40	0.039	0.50	0.013	Up	0.89
Cer d18:1/16:0	−0.11	0.585	0.02	0.935	Up	0.88
TG 16:1/14:1/18:2	0.18	0.377	0.07	0.731	Up	/
TG 16:0/17:0/18:2	−0.13	0.524	−0.14	0.519	Down	/
MG 18:2p	−0.01	0.947	−0.13	0.557	Up	/
DG 18:2/18:2	−0.43	0.026	−0.16	0.443	Up	/
PE 18:1p/22:6	0.10	0.614	0.16	0.460	Up	/
TG 18:0e/16:0/18:1	−0.25	0.209	−0.05	0.834	Up	/
DG 18:0/18:0	0.32	0.100	0.15	0.478	Up	/
Cer d18:1/22:0	0.11	0.579	0.17	0.433	Up	/
TG 18:1/17:1/18:2	0.10	0.624	0.15	0.498	Down	/
TG 18:2/17:1/18:2	0.35	0.076	0.46	0.023	Down	/
TG 8:0/10:0/10:0	0.33	0.096	0.00	0.987	Up	/
Cer d18:2/22:0	−0.04	0.836	0.15	0.476	Up	/
Chol	0.13	0.510	0.09	0.692	Up	/
PC 16:0/20:4	0.61	0.001	0.23	0.271	Up	/
PE 18:0p/18:1	0.16	0.413	0.27	0.205	Up	/
SM d41:1	−0.14	0.473	−0.21	0.324	Down	/
TG 15:0/16:0/18:2	−0.58	0.002	−0.51	0.011	Up	/
TG 15:0/18:2/18:2	−0.35	0.072	−0.38	0.067	Down	/
TG 16:0/14:0/16:1	−0.12	0.536	−0.15	0.491	Down	/
TG 16:0/18:1/22:5	0.55	0.003	0.36	0.087	Up	/
TG 16:0/18:2/22:6	0.28	0.152	0.42	0.043	Up	/
TG 16:1/18:2/18:3	0.48	0.011	0.43	0.035	Down	/
TG 17:0/18:1/18:2	0.13	0.534	0.08	0.719	Down	/

(*Continued*)

Table 3. Continued

Lipid Species	EAT vs HDL		EAT vs VLDL		EAT CAD vs NCAD	EAT CAD vs NCAD
	r	*P* Value	r	*P* Value	Regulation	Significative VIP
TG 18:0/16:0/17:0	0.46	0.015	0.37	0.079	Up	/
TG 18:0/16:0/18:0	0.51	0.007	0.27	0.201	Up	/
TG 18:3/18:2/18:2	0.24	0.224	0.32	0.125	Up	/
TG 8:0/8:0/10:0	−0.07	0.746	−0.27	0.200	Up	/
TG 8:0/8:0/8:0	−0.04	0.856	−0.14	0.527	Up	/

CAD indicates coronary artery disease; Cer, ceramide; Chol, cholesterol; Co, co-enzyme; DG, diglycerides; e, ether; EAT, epicardial adipose tissue; HDL, high-density lipoprotein; MG, monoglycerides; p, plasmalogen; PC, phosphatidylcholine; PE, phosphatidylethanolamine; PG, phosphatidylglycerol; SM, sphingomyelin; TG, triglycerides; VIP, variable importance in the projection value; and VLDL, very low-density lipoprotein.

coronary vasospasm, or intimal lesions. This provides evidence that bioactive molecules from the pericoronary tissues may alter arterial homeostasis.[38] These observations tended to support the concept of outside-to-inside cellular cross-talk in that inflammatory mediators or FFAs produced by EAT adjacent to the coronary artery, may have a paracrine toxic effect on the vasculature, in diffusing passively or via vasa vasorum through the vessel wall.[3] Using a pangenomic approach, we previously identified that EAT was particularly enriched in inflammation, extracellular matrix remodeling, immune signaling, thrombosis, beiging, coagulation, and apoptosis pathways.[39] Moreover, we demonstrated that Secretory Type II Phospholipase A2, which catalyzes the rate-limiting step in formation of proinflammatory lipid mediators, was highly expressed and secreted in the EAT of patients with CAD.[40] In this study, we bring further evidence that EAT is specifically enriched in ceramides, compared to SAT and in the context of CAD (in particular Cer d18). Ceramides are precursors for the predominant sphingolipids in the cell, including sphingomyelin and gangliosides. Sphingolipids are not absorbed from dietary sources but are instead produced from breakdown products of saturated fats (ie, palmitate) and proteins (ie, serine) via the action of serine palmitoyltransferase.[41] Many of them play important roles in cellular growth and function, with ceramides receiving the greatest attention, as they participate in numerous inflammatory processes, and have been found to disrupt insulin sensitivity, impair β-cell function, vascular reactivity, or mitochondrial metabolism, inducing cellular dysfunction, and apoptosis (lipotoxicity).[41,42] Ceramide 1-phosphate has been shown to mediate inflammatory responses by promoting phospholipase A2-mediated eicosanoid storm and by inducing cytokine production.[43,44] Ceramides activate the nucleotide-binding domain, leucine-rich-containing family, pyrin domain-containing-3 NLRP3 inflammasome, which activates caspase 1 and mediates the processing and release of IL-1β, the expression of which in EAT was predictive of CAD.[11,45] Acute generation of ceramide by sphingomyelinases is able to induce lipoproteins aggregation.[46] Ceramide is also implicated in oxidized LDL transcytosis across endothelial cells, thus being implicated in the retention of bioactive lipids in the vascular wall.[47] Last, endogenous ceramides regulate monocyte adhesion to vessel walls and then promotes atheroma plaque development.[48] Interestingly, the treatment of apo-E deficient mice with myriocin, the serine palmitoyltransferase inhibitor, and subsequent de novo ceramide synthesis, resulted in the 40% lowering of preformed atherosclerotic lesions.[49] These data are consistent with a specific role of ceramide in lipid-induced atherogenesis and inflammation. These lipids within the adipose tissue may participate in the induction of EAT inflammation, may also directly modulate vascular inflammation by outside-to-inside cellular cross-talk. Finally, they may directly act on myocardium (as there is no fascia separating epicardial adipocytes from cardiomyocytes) to participate in inflammation and modulate heart function.[41,42]

In this study, we identified specific lipidomic signature of isolated VLDL in CAD. VLDL from patients with CAD showed higher content of total lysophosphopholipids with lower content of monoglyceride (18:2p). However, no differences in the total content of each lipid in HDL were observed between patients with and without CAD. Remarkably, we observed that the EAT lipidome in CAD was only partially reflected by the plasma lipoproteins (HDL and VLDL) lipidome. Only 51 lipid species were found in common between EAT and plasma lipoproteins, and only 5 lipid species were correlated between EAT and isolated plasma VLDL or HDL. These data indicate that plasma isolated lipoproteins lipidomic profile does not entirely reflect the EAT lipidome and cannot be used as EAT bioactive lipid content biomarker.

Several limitations of our study should be noted. This was an observational study, with patients with CAD exhibiting more cardiovascular risk factors (smoking, diabetes mellitus, and higher TGs) than patients without CAD. These differences may have influenced our results. Some authors reported reduction in fatty acid (16:0) and an increase in (18:0, and conjugated linoleic acid) and a decrease of (18:1n-11, 20:5n-3, and 22:6n-3) in the EAT of diabetics.[9] Others have found a positive association between EAT volume and density (which reflects the tissue cellularity), diabetes mellitus, and active smoking.[50] Finally, Błachnio-Zabielska et al,[33] specifically described the bioactive lipids content of SAT and EAT in obese

diabetic, compared to lean nondiabetic, and obese nondiabetic subjects and found a positive correlation between C16:0-CoA content and HOMA-IR in EAT.[33] While we have discussed the evidence for a potential pathogenic role of bioactive lipids within EAT in CAD, future studies are needed to determine whether these lipids dynamically change the physiology of the arterial wall and are directly implicated in the development of atherogenesis.

Future Directions

This study brings new insight in the importance of ectopic adipose tissue lipids compared to classical plasma lipids in CAD pathophysiology. Future studies should focus on the characterization of these ectopic lipids and their role in inflammatory processes or thermogenesis. The development of new imaging techniques to assess non invasively EAT is warranted to ameliorate clinical practices and improve personalized medicine.

Conclusions

In this study, we uniquely demonstrated that CAD is associated with a specific lipidomic signature of EAT, unlike SAT, with a specific enrichment in ceramides, diglycerides monoglycerides, and less unsaturated TGs than patients without CAD. This increase in lipotoxic lipids could participate in the inflammation of the adjacent coronary artery wall and in the pathophysiology of CAD. Furthermore, we observed that the EAT lipidome in CAD was only partially reflected by the plasma lipoproteins (HDL and VLDL) lipidome, suggesting that plasma lipidome is not the biomarker of this ectopic dynamic organ.

ARTICLE INFORMATION

Received December 9, 2019; accepted February 4, 2020.

Affiliations

From the Universidad de Buenos Aires, Facultad de Farmacia y Bioquímica, Instituto de Fisiopatología y Bioquímica Clínica (INFIBIOC), Departamento de Bioquímica Clínica, Laboratorio de Lípidos y Aterosclerosis, Buenos Aires, Argentina (M.B., V.M., G.L., L.S., G.B.); Aix-Marseille University, INSERM, INRAE, C2VN, France (A.D., P.A., L.S., R.V., S.B., J.C.M., B.G.); Endocrinology, Metabolic Diseases and Nutrition Department, Assistance Publique Hôpitaux de Marseille, France (A.D., R.V., S.B., B.G.); CRIBIOM, Criblage Biologique Marseille, Faculté de Medecine de la Timone, France (L.S.); Universidad de Buenos Aires, CONICET, Facultad de Farmacia y Bioquímica, Argentina (V.M., G.B.); Universidad de Buenos Aires, Hospital de Clínicas "José de San Martín", División de Cirugía Cardiovascular, Argentina (M.R.); and Servicio de Docencia e Investigación, Hospital Central de Formosa, Facultad de Ciencias de la Salud, Universidad Nacional de Formosa, Argentina (J.P.N.).

Disclosures

None.

REFERENCES

1. Xu G, Liu B, Sun Y, Du Y, Snetselaar LG, Hu FB, Bao W. Prevalence of diagnosed type 1 and type 2 diabetes among US adults in 2016 and 2017: population based study. *BMJ*. 2018;362:k1497. doi:10.1136/bmj.k1497
2. Després JP. Body fat distribution and risk of cardiovascular disease: an update. *Circulation*. 2012;126:1301–1313. doi: 10.1161/CIRCULATIONAHA.111.067264
3. Gaborit B, Sengenes C, Ancel P, Jacquier A, Dutour A. Role of epicardial adipose tissue in health and disease: a matter of fat? *Compr Physiol*. 2017;7:1051–1082. doi: 10.1002/cphy.c160034
4. Mazurek T, Zhang L, Zalewski A, Mannion JD, Diehl JT, Arafat H, Sarov-Blat L, O'Brien S, Keiper EA, Johnson AG, et al. Human epicardial adipose tissue is a source of inflammatory mediators. *Circulation*. 2003;108:2460–2466. doi: 10.1161/01.CIR.0000099542.57313.C5
5. Iacobellis G. Local and systemic effects of the multifaceted epicardial adipose tissue depot. *Nat Rev Endocrinol*. 2015;11:363–371. doi: 10.1038/nrendo.2015.58
6. Marchington JM, Pond CM. Site-specific properties of pericardial and epicardial adipose tissue: the effects of insulin and high-fat feeding on lipogenesis and the incorporation of fatty acids *in vitro*. *Int J Obes*. 1990;14:1013–1022.
7. Rabkin SW. Epicardial fat: properties, function and relationship to obesity. *Obes Rev*. 2007;8:253–261. doi: 10.1111/j.1467-789X.2006.00293.x
8. Pezeshkian M, Noori M, Najjarpour-Jabbari H, Abolfathi A, Darabi M, Darabi M, Shaaker M, Shahmohammadi G. Fatty acid composition of epicardial and subcutaneous human adipose tissue. *Metab Syndr Relat Disord*. 2009;7:125–131. doi: 10.1089/met.2008.0056
9. Pezeshkian M, Mahtabipour MR. Epicardial and subcutaneous adipose tissue fatty acids profiles in diabetic and non-diabetic patients candidate for coronary artery bypass graft. *Bioimpacts*. 2013;3:83–89. doi: 10.5681/bi.2013.004
10. Mahabadi AA, Berg MH, Lehmann N, Kälsch H, Bauer M, Kara K, Dragano N, Moebus S, Jöckel KH, Erbel R, et al. Association of epicardial fat with cardiovascular risk factors and incident myocardial infarction in the general population: the Heinz Nixdorf Recall Study. *J Am Coll Cardiol*. 2013;61:1388–1395. doi: 10.1016/j.jacc.2012.11.062
11. Shimabukuro M, Hirata Y, Tabata M, Dagvasumberel M, Sato H, Kurobe H, Fukuda D, Soeki T, Kitagawa T, Takanashi S, et al. Epicardial adipose tissue volume and adipocytokine imbalance are strongly linked to human coronary atherosclerosis. *Arterioscler Thromb Vasc Biol*. 2013;33:1077–1084. doi:10.1161/ATVBAHA.112.300829
12. Quehenberger O, Armando AM, Brown AH, Milne SB, Myers DS, Merrill AH, Bandyopadhyay S, Jones KN, Kelly S, Shaner RL, et al. Lipidomics reveals a remarkable diversity of lipids in human plasma. *J Lipid Res*. 2010;51:3299–3305. doi: 10.1194/jlr.M009449
13. Quehenberger O, Dennis EA. The human plasma lipidome. *N Engl J Med*. 2011;365:1812–1823. doi: 10.1056/NEJMra1104901
14. American Diabetes Association. 2. Classification and diagnosis of diabetes: standards of medical care in diabetes-2019. *Diabetes Care*. 2019;42:S13–S28. doi:10.2337/dc19-S002
15. Schumaker VN, Puppione DL. Sequential flotation ultracentrifugation. *Methods Enzymol*. 1986;128:155–170. doi: 10.1016/0076-6879(86)28066-0
16. Barchuk M, Schreier L, López G, Cevey A, Baldi J, Fernandez Tomé MDC, Goren N, Rubio M, Miksztowicz V, Berg G. Glycosylphosphatidylinositol-anchored high density lipoprotein-binding protein 1 and angiopoietin-like protein 4 are associated with the increase of lipoprotein lipase activity in epicardial adipose tissue from diabetic patients. *Atherosclerosis*. 2019;288:51–59. doi: 10.1016/j.atherosclerosis.2019.06.915
17. Matyash V, Liebisch G, Kurzchalia TV, Shevchenko A, Schwudke D. Lipid extraction by methyl-tert-butyl ether for high-throughput lipidomics. *J Lipid Res*. 2008;49:1137–1146. doi: 10.1194/jlr.D700041-JLR200
18. Breitkopf SB, Ricoult SJH, Yuan M, Xu Y, Peake DA, Manning BD, Asara JM. A relative quantitative positive/negative ion switching method for untargeted lipidomics via high resolution LC-MS/MS from any biological source. *Metabolomics*. 2017;13:30. doi:10.1007/s11306-016-1157-8
19. Aidoud N, Delplanque B, Baudry C, Garcia C, Moyon A, Balasse L, Guillet B, Antona C, Darmaun D, Fraser K, et al. A combination of lipidomics, MS imaging, and PET scan imaging reveals differences in cerebral activity in rat pups according to the lipid quality of infant formulas. *FASEB J*. 2018;32:4776–4790. doi: 10.1096/fj.201800034R
20. Giacomoni F, Le Corguillé G, Monsoor M, Landi M, Pericard P, Pétéra M, Duperier C, Tremblay-Franco M, Martin JF, Jacob D, et al. Workflow4Metabolomics: a collaborative research infrastructure for computational metabolomics. *Bioinformatics*. 2015;31:1493–1495. doi: 10.1093/bioinformatics/btu813
21. Xia J, Psychogios N, Young N, Wishart DS. MetaboAnalyst: a web server for metabolomic data analysis and interpretation. *Nucleic Acids Res*. 2009;37(Web Server issue):W652–W660. doi: 10.1093/nar/gkp356

22. Papamandjaris AA, MacDougall DE, Jones PJ. Medium chain fatty acid metabolism and energy expenditure: obesity treatment implications. *Life Sci.* 1998;62:1203–1215. doi: 10.1016/s0024-3205(97)01143-0
23. Park H, He A, Tan M, Johnson JM, Dean JM, Pietka TA, Chen Y, Zhang X, Hsu FF, Razani B, et al. Peroxisome-derived lipids regulate adipose thermogenesis by mediating cold-induced mitochondrial fission. *J Clin Invest.* 2019;129:694–711. doi: 10.1172/JCI120606
24. Park H, He A, Lodhi IJ. Lipid regulators of thermogenic fat activation. *Trends Endocrinol Metab.* 2019;30:710–723. doi: 10.1016/j.tem.2019.07.020
25. Sacks HS, Fain JN, Bahouth SW, Ojha S, Frontini A, Budge H, Cinti S, Symonds ME. Adult epicardial fat exhibits beige features. *J Clin Endocrinol Metab.* 2013;98:E1448–E1455. doi: 10.1210/jc.2013-1265
26. Sacks HS, Fain JN, Holman B, Cheema P, Chary A, Parks F, Karas J, Optican R, Bahouth SW, Garrett E, et al. Uncoupling protein-1 and related messenger ribonucleic acids in human epicardial and other adipose tissues: epicardial fat functioning as brown fat. *J Clin Endocrinol Metab.* 2009;94:3611–3615. doi: 10.1210/jc.2009-0571
27. Baker RC, Nikitina Y, Subauste AR. Analysis of adipose tissue lipid using mass spectrometry. *Methods Enzymol.* 2014;538:89–105. doi: 10.1016/B978-0-12-800280-3.00006-2
28. Meex RC, Schrauwen P, Hesselink MK. Modulation of myocellular fat stores: lipid droplet dynamics in health and disease. *Am J Physiol Regul Integr Comp Physiol.* 2009;297:R913–R924. doi: 10.1152/ajpregu.91053.2008
29. Tomášová P, Čermáková M, Pelantová H, Vecka M, Kratochvílová H, Lipš M, Lindner J, Šedivá B, Haluzík M, Kuzma M. Minor lipids profiling in subcutaneous and epicardial fat tissue using LC/MS with an optimized preanalytical phase. *J Chromatogr B Analyt Technol Biomed Life Sci.* 2019;1113:50–59. doi:10.1016/j.jchromb.2019.03.006
30. van Meer G, Voelker DR, Feigenson GW. Membrane lipids: where they are and how they behave. *Nat Rev Mol Cell Biol.* 2008;9:112–124. doi: 10.1038/nrm2330
31. Bambace C, Telesca M, Zoico E, Sepe A, Olioso D, Rossi A, Corzato F, Di Francesco V, Mazzucco A, Santini F, et al. Adiponectin gene expression and adipocyte diameter: a comparison between epicardial and subcutaneous adipose tissue in men. *Cardiovasc Pathol.* 2011;20:e153–e156. doi: 10.1016/j.carpath.2010.07.005
32. Jové M, Moreno-Navarrete JM, Pamplona R, Ricart W, Portero-Otín M, Fernández-Real JM. Human omental and subcutaneous adipose tissue exhibit specific lipidomic signatures. *FASEB J.* 2014;28:1071–1081. doi: 10.1096/fj.13-234419
33. Błachnio-Zabielska AU, Baranowski M, Hirnle T, Zabielski P, Lewczuk A, Dmitruk I, Górski J. Increased bioactive lipids content in human subcutaneous and epicardial fat tissue correlates with insulin resistance. *Lipids.* 2012;47:1131–1141. doi: 10.1007/s11745-012-3722-x
34. Gaborit B, Kober F, Jacquier A, Moro PJ, Flavian A, Quilici J, Cuisset T, Simeoni U, Cozzone P, Alessi MC, et al. Epicardial fat volume is associated with coronary microvascular response in healthy subjects: a pilot study. *Obesity (Silver Spring).* 2012;20:1200–1205. doi:10.1038/oby.2011.283
35. Mancio J, Azevedo D, Saraiva F, Azevedo AI, Pires-Morais G, Leite-Moreira A, Falcao-Pires I, Lunet N, Bettencourt N. Epicardial adipose tissue volume assessed by computed tomography and coronary artery disease: a systematic review and meta-analysis. *Eur Heart J Cardiovasc Imaging.* 2018;19:490–497. doi:10.1093/ehjci/jex314
36. Cheng KH, Chu CS, Lee KT, Lin TH, Hsieh CC, Chiu CC, Voon WC, Sheu SH, Lai WT. Adipocytokines and proinflammatory mediators from abdominal and epicardial adipose tissue in patients with coronary artery disease. *Int J Obes (Lond).* 2008;32:268–274. doi: 10.1038/sj.ijo.0803726
37. Baker AR, Harte AL, Howell N, Pritlove DC, Ranasinghe AM, da Silva NF, Youssef EM, Khunti K, Davies MJ, Bonser RS, et al. Epicardial adipose tissue as a source of nuclear factor-kappaB and c-Jun N-terminal kinase mediated inflammation in patients with coronary artery disease. *J Clin Endocrinol Metab.* 2009;94:261–267. doi: 10.1210/jc.2007-2579
38. Shimokawa H, Ito A, Fukumoto Y, Kadokami T, Nakaike R, Sakata M, Takayanagi T, Egashira K, Takeshita A. Chronic treatment with interleukin-1 beta induces coronary intimal lesions and vasospastic responses in pigs in vivo. The role of platelet-derived growth factor. *J Clin Invest.* 1996;97:769–776. doi: 10.1172/JCI118476
39. Gaborit B, Venteclef N, Ancel P, Pelloux V, Gariboldi V, Leprince P, Amour J, Hatem SN, Jouve E, Dutour A, et al. Human epicardial adipose tissue has a specific transcriptomic signature depending on its anatomical peri-atrial, peri-ventricular, or peri-coronary location. *Cardiovasc Res.* 2015;108:62–73. doi: 10.1093/cvr/cvv208
40. Dutour A, Achard V, Sell H, Naour N, Collart F, Gaborit B, Silaghi A, Eckel J, Alessi MC, Henegar C, et al. Secretory type II phospholipase A2 is produced and secreted by epicardial adipose tissue and overexpressed in patients with coronary artery disease. *J Clin Endocrinol Metab.* 2010;95:963–967. doi: 10.1210/jc.2009-1222
41. Chaurasia B, Summers SA. Ceramides - Lipotoxic inducers of metabolic disorders. *Trends Endocrinol Metab.* 2015;26:538–550. doi: 10.1016/j.tem.2015.07.006
42. Aburasayn H, Al Batran R, Ussher JR. Targeting ceramide metabolism in obesity. *Am J Physiol Endocrinol Metab.* 2016;311:E423–E435. doi: 10.1152/ajpendo.00133.2016
43. Chiurchiù V, Leuti A, Maccarrone M. Bioactive lipids and chronic inflammation: managing the fire within. *Front Immunol.* 2018;9:38. doi: 10.3389/fimmu.2018.00038
44. Pettus BJ, Bielawska A, Subramanian P, Wijesinghe DS, Maceyka M, Leslie CC, Evans JH, Freiberg J, Roddy P, Hannun YA, et al. Ceramide 1-phosphate is a direct activator of cytosolic phospholipase A2. *J Biol Chem.* 2004;279:11320–11326. doi: 10.1074/jbc.M309262200
45. Vandanmagsar B, Youm YH, Ravussin A, Galgani JE, Stadler K, Mynatt RL, Ravussin E, Stephens JM, Dixit VD. The NLRP3 inflammasome instigates obesity-induced inflammation and insulin resistance. *Nat Med.* 2011;17:179–188. doi: 10.1038/nm.2279
46. Walters MJ, Wrenn SP. Mechanistic roles of lipoprotein lipase and sphingomyelinase in low density lipoprotein aggregation. *J Colloid Interface Sci.* 2011;363:268–274. doi: 10.1016/j.jcis.2011.07.072
47. Li W, Yang X, Xing S, Bian F, Yao W, Bai X, Zheng T, Wu G, Jin S. Endogenous ceramide contributes to the transcytosis of oxLDL across endothelial cells and promotes its subendothelial retention in vascular wall. *Oxid Med Cell Longev.* 2014;2014:823071. doi: 10.1155/2014/823071
48. Gao D, Pararasa C, Dunston CR, Bailey CJ, Griffiths HR. Palmitate promotes monocyte atherogenicity via de novo ceramide synthesis. *Free Radic Biol Med.* 2012;53:796–806. doi: 10.1016/j.freeradbiomed.2012.05.026
49. Hojjati MR, Li Z, Zhou H, Tang S, Huan C, Ooi E, Lu S, Jiang XC. Effect of myriocin on plasma sphingolipid metabolism and atherosclerosis in apoE-deficient mice. *J Biol Chem.* 2005;280:10284–10289. doi: 10.1074/jbc.M412348200
50. Milanese G, Silva M, Bruno L, Goldoni M, Benedetti G, Rossi E, Ferrari C, Grutta L, Maffei E, Toia P, et al. Quantification of epicardial fat with cardiac CT angiography and association with cardiovascular risk factors in symptomatic patients: from the ALTER-BIO (Alternative Cardiovascular Bio-Imaging markers) registry. *Diagn Interv Radiol.* 2019;25:35–41. doi: 10.5152/dir.2018.18037